Available online at www.sciencedirect.com
ScienceDirect
C. R. Physique 10 (2009) 414–422
COMPTES RENDUS PHYSIQUE

Metamaterials / Métamateriaux

Directive metamaterial-based subwavelength resonant cavity antennas – Applications for beam steering

Abdelwaheb Ourir, Shah Nawaz Burokur, Riad Yahiaoui, André de Lustrac *

Institut d'électronique fondamentale, Université Paris Sud, UMR 8622 – CNRS, 91405 Orsay cedex, France

Available online 26 June 2009

Abstract

This article presents the use of composite resonant metamaterials for the design of highly directive subwavelength cavity antennas. These metamaterials, composed of planar metallic patterns periodically organized on dielectric substrates, exhibit frequency dispersive phase characteristics. Different models of metamaterial-based surfaces (metasurfaces), introducing a zero degree reflection phase shift to incident waves, are firstly studied where the bandwidth and operation frequency are predicted. These surfaces are then applied in a resonant Fabry–Perot type cavity and a ray optics analysis is used to design different models of ultra-compact high-gain microstrip printed antennas. Another surface presenting a variable reflection phase by the use of a non-periodic metamaterial-based metallic strips array is designed for a passive low-profile steering beam antenna application. Finally, the incorporation of active electronic components on the metasurfaces, allowing an electronic control of the phase responses, is applied to an operation frequency reconfigurable cavity and a beam steering cavity. All these cavity antennas operate on subwavelength modes, the smallest cavity thickness being of the order of $\lambda/60$. ***To cite this article: A. Ourir et al., C. R. Physique 10 (2009).***

Résumé

Antennes directives à cavité résonante sub-longueur d'onde à métamatériaux – applications au dépointage. Cet article présente l'utilisation de métamatériaux composites résonants pour la conception d'antennes à cavités sub-longueurs d'onde hautement directives. Ces métamatériaux composés de motifs métalliques planaires disposés périodiquement sur des substrats diélectriques montrent des caractéristiques de phase dispersives en fréquence. Plusieurs types de surfaces à base de métamatériaux (métasurfaces), présentant une réflexion en phase avec l'onde incidente sont étudiés afin de calculer leurs largeurs de bande et leurs fréquences de travail. Ces surfaces sont ensuite appliquées à des cavités de type Fabry–Perot et une analyse basée sur un modèle de lancer de rayons est utilisée pour réaliser des antennes ultra-compactes et hautement directives. Une métasurface avec une phase à la réflexion variable obtenue avec des métamatériaux apériodiques est conçue pour des applications de dépointage passif de faisceau d'antennes. En dernier lieu, l'implantation de composants électroniques dans une métasurface contrôlable, permettant un contrôle électronique de la phase à la réflexion, est utilisée pour la conception de cavités reconfigurables en fréquence et de cavités à balayage de faisceau. Toutes ces antennes à cavités opèrent sur des modes sub-longueurs d'ondes avec des épaisseurs aussi faibles que $\lambda/60$. ***Pour citer cet article : A. Ourir et al., C. R. Physique 10 (2009).***

Keywords: Metamaterials; High directivity; Subwavelength; Fabry–Perot cavity antennas; Variable phase; Frequency reconfigurable; Beam steering

* Corresponding author.
E-mail address: andre.de-lustrac@u-psud.fr (A. de Lustrac).

1631-0705/$ – see front matter
doi:10.1016/j.crhy.2009.01.004

Mots-clés : Métamatériaux ; Haute directivité ; Sub-longueur d'onde ; Cavité Fabry–Perot ; Phase variable ; Reconfigurabilité en fréquence ; Balayage du faisceau

1. Introduction

High Impedance Surfaces (HIS) are passive metallic arrays organized on dielectric boards that were initially used for the suppression of surface wave propagation [1]. Over the last few years, this type of structure has been integrated in configurations that comprise small antennas in order to enhance their performances [1–3]. However, the HIS of Sievenpiper needs a non-planar fabrication process, which is not suitable for implementation in lots of microwave and millimetric circuits. Artificial Magnetic Conductors (AMC) composed of a planar periodic array of metallic patches without shorted vias to the ground plane exhibiting not only a high impedance, but also an exactly zero degree reflection phase at the resonance frequency, have been proposed for antenna and circuit applications [4–6]. These AMC surfaces were recently used by Feresidis et al. in order to achieve $\lambda/4$ thick resonant cavities [7]. In [8], we designed a subwavelength ($\lambda/60$) directive cavity by making use of a novel type of composite metamaterial-based Partially Reflecting Surface (PRS) constituted by simultaneously inductive and capacitive grids and an AMC surface acting as the feeding patch antenna's substrate. In 2005, D. Sievenpiper expanded the capabilities of HIS to perform active control of electromagnetic waves by implementing active components in the periodic patterns [9,10]. Another concept using active Left-Handed (LH) metamaterial was proposed for steerable antenna applications [11].

In this article, using a novel composite metamaterial, made of capacitive and inductive grids, we present several examples of low-profile and high-gain metamaterial-based cavity antennas. First we study a cavity of thickness $\lambda/30$ for applications to ultra-thin directive antennas using only one 1-D metamaterial-based surface acting as a PRS [12]. We then present the modelling and characterization of an optimized resonant cavity for a passive directive steered beam antenna near 10 GHz [13]. We then study an electronically active metamaterial-based subwavelength cavity for a frequency reconfigurable low-profile and high-gain antenna application. Finally, a numerical analysis of an electronically active beam steering cavity is presented, using the Transmission Line Matrix (TLM) method software *Microstripes* [14].

2. Passive subwavelength cavities based on metasurfaces

A cavity antenna is formed by a feeding source placed between two reflecting surfaces as shown in Fig. 1(a). In this paper, different cavities based on the model presented in Fig. 1(a) will be discussed and used. The cavity is composed of a Perfectly Electrically Conductive (PEC) surface acting as a conventional ground plane for the feeding source and a metamaterial-based surface (metasurface) playing the role of a transmitting window known as a PRS. Following the early work of Trentini [15], a simple optical ray model can be used to describe the resonant cavity modes. This model is used to theoretically predict the working mode of a low-profile high-directivity metamaterial-based subwavelength cavity antenna. Let us consider the cavity presented in Fig. 1(a). It is formed by a feeding antenna placed between two reflectors separated by a distance h. Phase shifts are introduced by these two reflectors and also by the path length of the wave traveling inside the cavity. With the multiple reflections of the wave emitted by the antenna, a resonance is achieved when the reflected waves are in phase after one cavity roundtrip. The resonance condition, for waves propagating vertically, can then be written as:

$$h = (\phi_{\mathrm{PRS}} + \phi_{\mathrm{r}})\frac{\lambda}{4\pi} - (n \times e) \pm N\frac{\lambda}{2} \tag{1}$$

where ϕ_{PRS} is the reflection phase of the PRS reflector, ϕ_{r} is the reflection phase of the feeding antenna's ground plane, n is the refractive index of the substrate and e its thickness. N is an integer qualifying the electromagnetic mode of the cavity. If the cavity and the substrate thicknesses e and h are fixed, the resonant wavelength is determined by the sum of the reflection phases $\phi_{\mathrm{PRS}} + \phi_{\mathrm{r}}$ for a fixed N. Conversely, for a given wavelength, the thickness h can be minimized by reducing the total phase shift $\phi_{\mathrm{PRS}} + \phi_{\mathrm{r}}$. The use of metasurfaces answers this purpose since they can exhibit an LC resonance. This resonance helps to have a reflection phase response varying from 180 to $-180°$, passing through $0°$ at the resonance frequency. As the reflector near the feeding antenna is composed of a PEC surface, then ϕ_{r} will be very close to $180°$. By choosing a correct working cavity frequency above the metasurface resonance

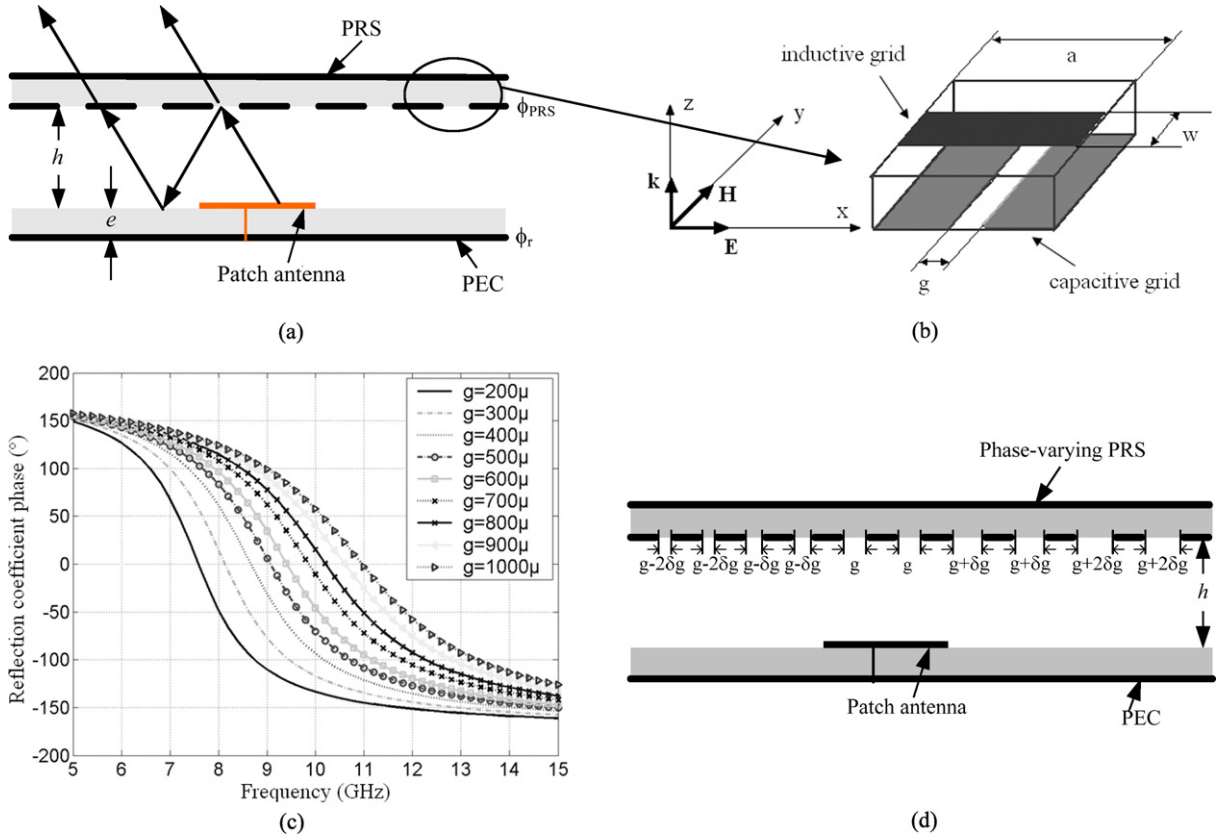

Fig. 1. (a) Schematic view of the cavity antenna composed of a PEC and a PRS metasurface. (b) Elementary cell of the metamaterial composed of an inductive and capacitive grid, which is proposed for the PRS. (c) Reflection phase coefficient of the metasurface versus the gap width g. (d) Schematic view of the cavity composed of a PEC and a metasurface with a variable gap width.

corresponding to a reflection phase close to $-180°$, the sum $\phi_{PRS} + \phi_r$ can be very small leading to a very low cavity thickness.

The composite 1-D metasurface consists of a periodic array of copper strips mechanically etched on each face of a 1.4 mm-thick FR3-epoxy ($\varepsilon_r = 3.9$ and $\tan\delta = 0.0197$) substrate as shown by the elementary cell in Fig. 1(b). The periodicity a and the width w of the strips are 5 and 2.2 mm respectively, optimized to have a resonance and to provide a sufficiently high reflectance near 10 GHz. The upper array where the strips are oriented parallel to the electric field **E** of the antenna plays the role of the inductive grid, whereas the lower array where the strips are oriented parallel to the magnetic field **H** acts as the capacitive grid. We shall note that the gap spacing g in the capacitive grid plays a crucial role in determining the capacitance and therefore the resonance frequency of the metasurface. By changing g and keeping all the other geometric parameters unchanged, the capacitance of the metamaterial will also vary. As a consequence, the phases of the computed reflection coefficients vary. This behaviour is illustrated by the simulation results shown in Fig. 1(c). We can note that the variation of g accounts for the shift of the resonance frequency. An increase in the value of g causes a decrease in the value of the capacitance created between two cells, and finally a shift of the resonance towards higher frequencies. At a particular frequency, the phase of the metasurface increases with an increase in the gap spacing. The study on the variation of g shows that it is possible to design a PRS with a continuous variation of the gap g, resulting in a local variation of the phase characteristics (Fig. 1(d)). If we consider each gap as a slot antenna, an analogy can then be made with an array of several antennas with a regular phase difference. The locally variable phase metasurface can then be applied for passive beam steering.

Several subwavelength cavities have been simulated and fabricated using the 1-D metasurface as PRS. Concerning the PRS, 11×11 unit cells have been used and therefore the overall dimensions of the prototypes are $55 \times 55 \times 3.8$ mm^3. The first one consists of the metamaterial PRS with the same gap spacing $g = 400$ µm between the metallic

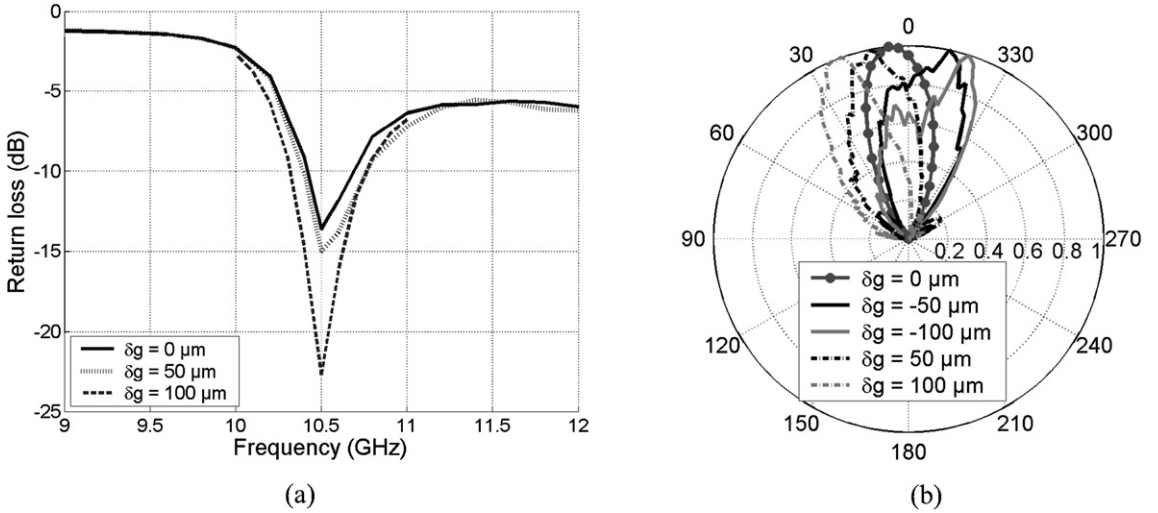

Fig. 2. (a) Return loss of the antennas with different variation of gap width. (b) Measured gain patterns of the cavity antennas versus the gap width variation.

strips of the capacitive grid ($\delta g = 0$). This prototype will assure no deflection of the beam since it exists no phase variation of the metamaterial. The second and third ones are the prototypes incorporating respectively a variation of $\delta g = 50$ μm and $\delta g = 100$ μm along the positive x-direction. The cases where the variation δg is negative (180° rotation of the PRS around the z-axis) have also been considered. Note that here the resonance frequency of the central region of the metamaterial corresponds to that of the PRS without gap spacing variation ($g = 400$ μm and $\delta g = 0$), i.e. 8.7 GHz as shown in Fig. 1(c). The resonance frequency of the cavity is found to be ∼10.5 GHz for the three prototypes as shown in Fig. 2(a). Best matching is observed when the metallic gap of the PRS capacitive grid increases. However, the resonance frequency remains the same for the three configurations since it depends on the gap spacing of the central region of the PRS, which is the same for the three prototypes.

Fig. 2(b) shows the measured gain patterns of the antenna in the E ($\phi = 90°$) plane at 10.5 GHz for an optimized cavity thickness $h = 1$ mm. For $\delta g = 0$, the beam is normal to the plane of the antenna and shows no deflection, which confirms our prediction on the constant phase metamaterial. However, in the case of a regular variation of 50 μm, a deflection of the antenna beam of about 10° can be observed either in the forward (clockwise) or backward (anti-clockwise) direction depending if δg is respectively negative or positive. Similar observations and a higher deflection of ±20° can be noted for $\delta g = \pm 100$ μm. The directivity of the cavity antenna can be calculated using the following expression: $D = 41253/(\theta_1 \times \theta_2)$ where θ_1 and θ_2 are respectively the half-power widths (in degrees) for the **H**-plane and **E**-plane patterns. In our case, the directivity is found to be approximately equal to 14.8 dB.

3. Electronically controllable cavity antenna

This section deals with the modeling and characterization of an active frequency reconfigurable subwavelength metamaterial-based cavity antenna. The aim of this active reconfigurable cavity is to be able to control dynamically the antenna's resonance frequency and beam steering. In literature, electronically controllable textured surfaces have been applied to leaky wave antennas [10] and radomes [11]. The tunable PRS used here is composed of a composite phase varying metamaterial, by the insertion of active electronic components, and is proposed for the design of firstly a frequency reconfigurable and secondly a controllable beam steering low-profile and high-gain Fabry–Perot cavity antenna. The study and design of this active phase-varying metamaterial tunable metasurface used as a PRS are described before presenting the two different operating modes.

3.1. Electronically phase-varying metasurface

The metasurface used in this section is based on the same principle as the one illustrated in Fig. 1(d). But, instead of applying a linear variation of the gap spacing g in order to create a locally variable phase, we now use active

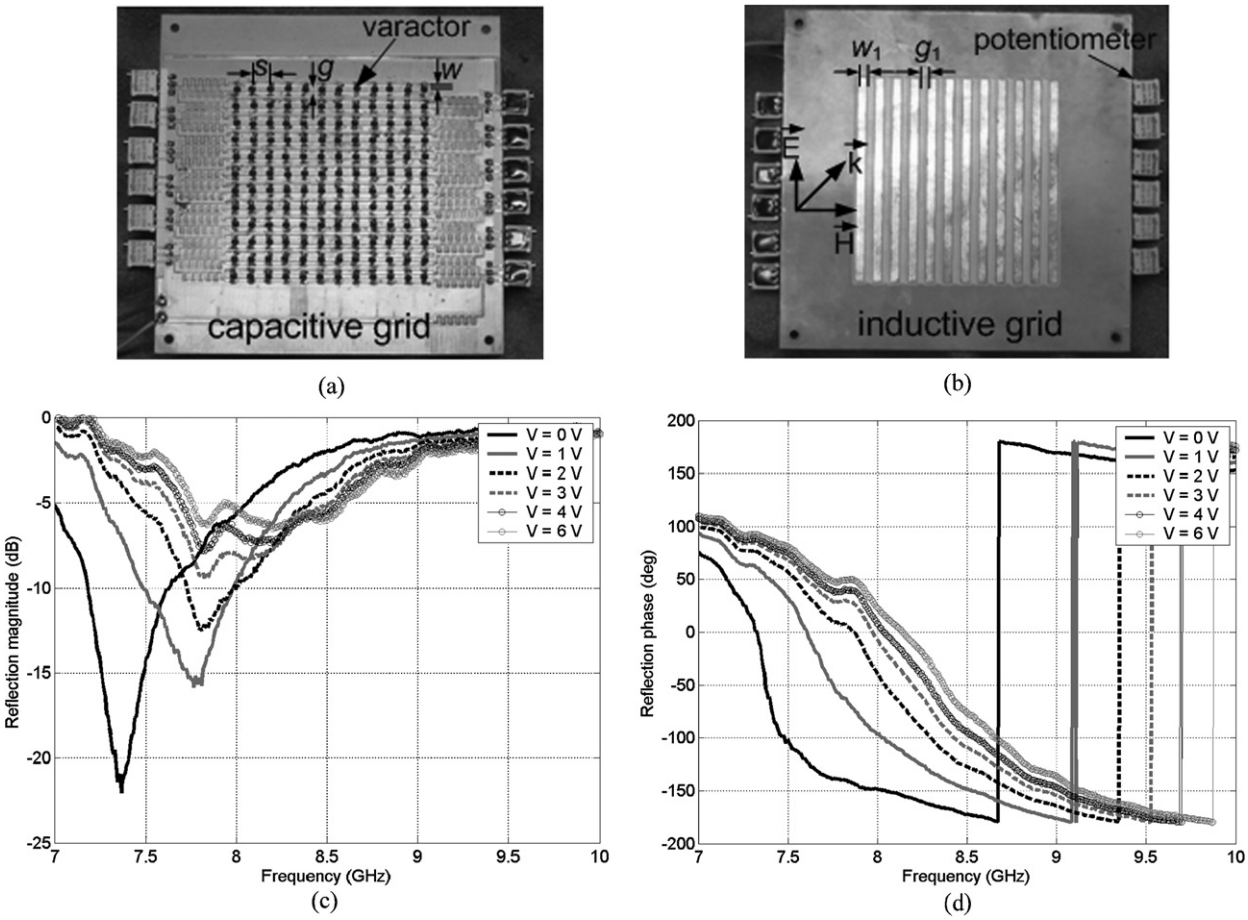

Fig. 3. Electronically phase-varying metasurface. (a) Capacitive grid incorporating varactors and voltage dividers. (b) Inductive grid. (c) Measured magnitude and (d) measured phase of the reflection coefficient versus the bias of the varicaps.

components to make the phase of the metasurface shift in frequency. Varactor diodes having a capacitance value ranging from 0.5 pF to 1.0 pF are thus incorporated into the capacitive grid between two adjacent metallic strips (Fig. 3(a)) and depending on the applied bias voltage, the phase of the metasurface varies with frequency. The variable capacitive grid of the tunable phase PRS used for this work consists of a lattice of metallic strips with varactor diodes connected each 6 mm ($s = 6$ mm) between two adjacent strips. The width of the strips and the spacing between two strips of the capacitive grid is respectively $w = 1$ mm and $g = 2$ mm (Fig. 3(a)). Concerning the inductive grid, the width of the strips and the spacing between two strips are respectively $w_1 = 2$ mm and $g_1 = 4$ mm (Fig. 3(b)). Note that the inductive grid is not made tunable. RF inductances are also used in the microstrip circuit in order to prevent high frequency signals going to the DC system. Potentiometers are implemented in the structure to create a voltage divider circuit so as to be able to bias locally the varactors. A prototype is designed and fabricated where the capacitance in each row can be adjusted according to the bias voltage applied. This capacitance can also be varied from one row to another by the use of the voltage dividers on the prototype. By changing the bias voltage of the varactors of the PRS similarly, the capacitance of the metamaterial will also vary. As a consequence, the reflection and the transmission coefficients also vary. This behaviour is illustrated by the measurement results of the reflection coefficient magnitude and phase shown in Figs. 3(c) and 3(d) respectively. These curves are obtained when the same bias voltage is applied to the different rows of varactors along the PRS. The measurements are performed in an anechoic chamber using two horn antennas working in the [2 GHz–18 GHz] frequency band and an 8722ES network analyzer. From Fig. 2(a), we can note that the variation of the bias voltage accounts for the shift of the resonance frequency of the PRS, i.e. the frequency where the phase crosses 0°. An increase in the bias voltage leads to a decrease in the value of the capacitance of the metamaterial, and finally to a shift of the resonance towards higher frequencies. At a particular

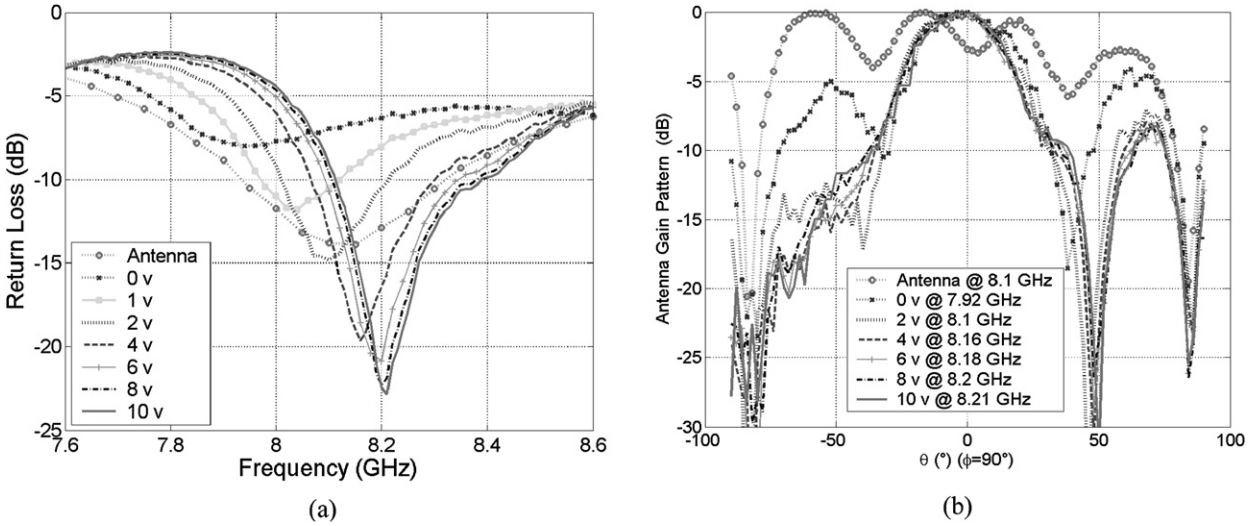

Fig. 4. Electronically frequency reconfigurable cavity antenna. (a) Return losses. (b) **E**-plane ($\phi = 90°$) radiation patterns.

frequency the phase of the PRS increases with an increase in the bias voltage. This phase shift is very important since it will help to tune the resonance frequency of the cavity antenna and also to control the radiated beam direction of the antenna.

3.2. Electronically frequency reconfigurable cavity antenna

The PRS studied above is placed at a distance $h = 0.5$ mm above a rectangular patch antenna with dimensions 9×9 mm^2 acting as the cavity feeding source to design a subwavelength Fabry–Perot cavity. The patch antenna alone has a resonance frequency of 8.1 GHz. A prototype of the subwavelength cavity is fabricated. The resonance frequency of the proposed cavity, which depends on the phase of the reflection coefficient of the PRS and also the height, is found to be in the vicinity of 8 GHz for the different bias voltages applied. Fig. 4(a) shows the matching of the cavity antenna with different bias voltage of the varactors. In this working mode all the biases of the varicaps are identical and are changed simultaneously. Two important observations are made and are illustrated in this figure. Firstly, as for the reflection phase response, a shift towards high frequencies of the cavity resonance is noted when the bias voltage varies from 0 V to 10 V. This is due to the decrease in the capacitance of the PRS. The shift in frequency is explained by Eq. (1). In this equation, we can see that if we keep h fixed and vary the sum of phases, the working resonance wavelength and therefore the resonance frequency changes. Moreover, it can be observed that the dip of the resonance increases when the bias voltage is tuned from 0 V to 10 V, indicating an enhancement of the matching of the cavity. This enhancement is explained by the fact that the cavity antenna is better and better matched for the thickness $h = 0.5$ mm fixed when the bias voltage varies from 0 V to 10 V. If we change the thickness h of the cavity, we obtain a better matching at another frequency since the resonance frequency depends on the reflection phase of the PRS as well as the cavity thickness h as shown in the relation given by Eq. (1) for the resonance condition.

Measurements of the radiation patterns of the reconfigurable cavity antenna are done in the anechoic chamber and are presented in Fig. 4(b). The diagrams in the **E**-planes are plotted for the case of the microstrip patch antenna alone and for the cavity antenna at different frequencies corresponding to the best matching obtained when the bias voltage is changed (see Fig. 4(a)). When the capacitance of the PRS changes by a variation of the bias voltage of the varactors, a better directivity is obtained for the metamaterial-based cavity antenna compared to the case of the antenna alone. A -3dB beamwidth of 45° is thus observed for the cavity antenna instead of more than 100° for the microstrip antenna alone. However, we can note from this figure that a secondary lobe with quite a high level appears on the radiation pattern. This high magnitude may be probably due to a high coupling between the metamaterial-based PRS and the feeding antenna. An optimization of this cavity should reduce the level of this secondary lobe and enhance the performances. The directivity of the cavity antenna calculated is found to be approximately equal to 14.85 dB.

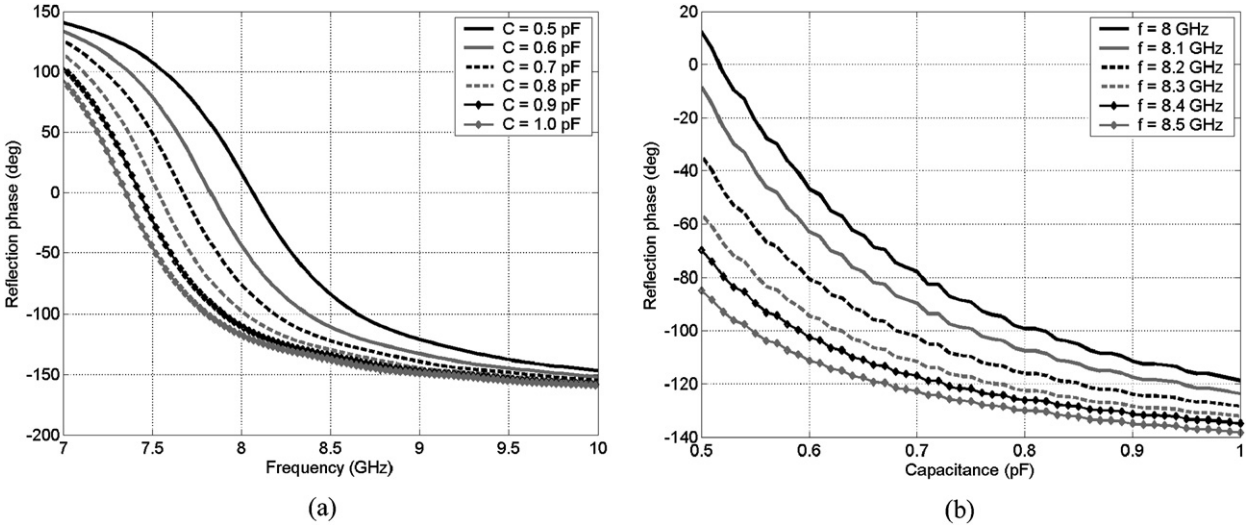

Fig. 5. Locally phase varying metasurface. (a) Reflection phase coefficient for different capacitance values from 0.5 pF to 1.0 pF. (b) Reflection phase versus capacitance for different frequencies.

3.3. Electronically controllable beam steering

Our approach here is based on a cavity antenna using a metasurface with a locally variable phase acting as a Partially Reflective Surface. Instead of applying a uniform variation in the periodicity of the cells composing the capacitive grid so as to create a locally variable phase as in Section 2, we now use active components to achieve this particular local phase variation of the PRS. The active components biased differently make the phase of the PRS shifts in frequency locally. For this study, simulations are firstly carried out on the unit cell of the metasurface for different capacitance value. Fig. 5(a) shows the reflection phase coefficient for different capacitance values from 0.5 pF to 1.0 pF. From Fig. 5(a), the reflection phase coefficient versus capacitance value is then derived for a considered frequency band lying from 8 GHz to 8.5 GHz. These phase-capacitance characteristics presented in Fig. 5(b) are used to determine the capacitance value for a desired phase shift between each cell on the metasurface.

The cavity considered here is composed of the patch antenna's PEC ground plane and of the PRS reflector presented above placed at a distance $h = 3$ mm ($\lambda/12$ at 8 GHz). As illustrated by the varactors bias system shown in Fig. 6(a), the proposed PRS is now divided into different regions, where each of them has a specific voltage bias. We shall note that here the resonance frequency of the cavity is imposed by the resonance frequency of the central region just above the feeding source corresponding to the bias voltage $V_4 = V_1 + 3\delta V$. The bias voltage is thus increased uniformly with a step δV when moving from the left to the right of the metamaterial-based PRS by the use of the potentiometers. This action creates a regular variation of the phase along the PRS.

The first configuration studied here is the antenna cavity based on the metamaterial PRS with the same null bias voltage for all the varactors. This configuration will assure no deflection of the beam, since there exists no phase variation of the metamaterial. The second and third configurations are prototypes incorporating respectively a variation of $\delta V = 0.2$ V and $\delta V = 0.3$ V along the positive x-direction. The cases where the variation δV is negative (180° rotation of the PRS around the z-axis) have also been considered.

Fig. 6(b) shows the gain patterns of the antenna in the **E**-plane ($\phi = 90°$) at 7.9 GHz for the optimized cavity thickness $h = 3$ mm. For $\delta V = 0$ V, the beam is normal to the plane of the antenna and shows no deflection, which confirms our prediction on the constant phase metamaterial. However, in the case of a regular variation of $\delta V = 0.2$ V, a deflection of the antenna beam of about 7° can be observed either in the forward or backward direction depending if δV is respectively negative or positive. Similar observations and a higher deflection can be noted for respectively $\delta V = 0.3$ V and $\delta V = -0.3$ V. This figure illustrates very clearly the control of the radiation pattern of the antenna by the bias of the varactors. The direction of the radiation beam depends of the direction of the variation of the bias of the varactors. If we inverse the sign of δV, the sign of the deviation changes also. This demonstration opens the door to the realization of very simple electronically beam steering ultra-compact antennas based on active metamaterials.

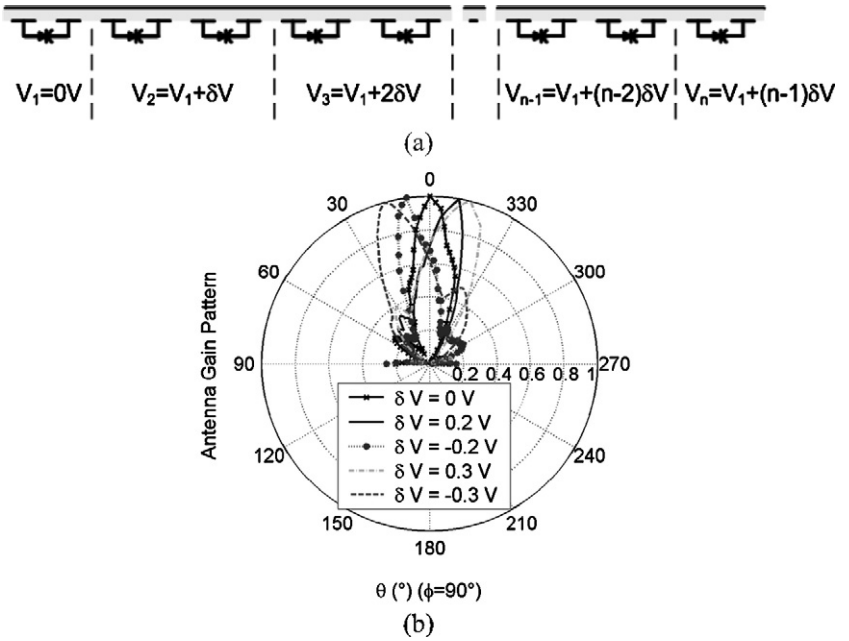

Fig. 6. (a) Variation of the bias voltage of the varactors along the phase varying PRS. (b) Measured gain patterns in the **E**-plane ($\phi = 90°$) at 7.9 GHz for $\delta V = 0$ V, $\delta V = 0.2$ V and $\delta V = 0.3$ V. The steering of the antenna's radiated beam can be clearly observed with a positive steering angle for positive bias and negative one for a negative bias.

4. Conclusion

Subwavelength metamaterial-based planar surfaces are used for applications to ultra-compact directive reconfigurable cavity antennas. Two types of metamaterial-based cavities are proposed. The first one consists in using a new passive locally phase-varying metamaterial-based PRS. It is proposed for applications where the radiated beam can be passively steered into a desired direction. This phase-varying PRS is composed of inductive and capacitive strips and by varying the capacitance locally with a continuous variation of the gap between the capacitive strips, a variable phase is achieved. A fabricated compact steerable directive cavity antenna of thickness $\lambda/30$ shows the possibility of obtaining a deflection of the beam of $\pm 20°$. In a second cavity, an electronically tunable metasurface is proposed as the PRS for the design of a tunable frequency and active beam steering cavity. This metasurface is made of a constant inductive grid and an active capacitive grid designed by the insertion of varactors. The negative reflection phase exhibited by the metamaterial combined with the phase at the surface of the feeding antenna's substrate (very close to 180°) above a conventional ground plane leads to the design of a frequency reconfigurable sub-wavelength cavity by tuning the bias voltage of all the varactors similarly. Furthermore, by applying a regular increase in the varactor bias voltages between the metallic strips of the capacitive grid in one direction, the phases of the reflection and transmission coefficients vary locally. As a consequence, the steering of the radiated beam can be controlled electronically. This proposed active cavity antenna can provide a low-cost ultra-compact alternative to traditional electrically scanned antennas.

Acknowledgement

This work was supported in part by the European Eureka TELEMAC project and by the French National Research Agency (ANR) METABIP project.

References

[1] D. Sievenpiper, L. Zhang, R.F.J. Broas, N.G. Alexópoulos, E. Yablonovitch, High-impedance electromagnetic surfaces with a forbidden frequency band, IEEE Trans. Microw. Theory Tech. 47 (11) (1999) 2059–2074.

[2] R.F.J. Broas, D. Sievenpiper, E. Yablonovitch, A high-impedance ground plane applied to a cellphone handset geometry, IEEE Trans. Microw. Theory Tech. 49 (7) (2001) 1262–1265.

[3] L. Zhou, H. Li, Y. Qin, Z. Wei, C.T. Chan, Directive emissions from subwavelength metamaterial-based cavities, Appl. Phys. Lett. 86 (2005) 101101.
[4] D.M. Pozar, S.D. Targonski, H.D. Syrigos, Design of millimeter wave microstrip reflectarrays, IEEE Trans. Antennas and Propagation 45 (2) (1997) 287–296.
[5] F.-R. Yang, K.-P. Ma, Y. Qian, T. Itoh, Aperture-coupled patch antennas on uc-pbg substrate, IEEE Trans. Microw. Theory Tech. 47 (11) (1999) 2123–2130.
[6] F.-R. Yang, Y. Qian, T. Itoh, Antenna and circuit applications of uc-pbg structures, in: Proc. Int. Symp. Dig. on Antennas and Propagation, ISAP, 2000, pp. 775–778.
[7] A.P. Feresidis, G. Goussetis, S. Wang, J.C. Vardaxoglou, Artificial magnetic conductor surfaces and their application to low-profile high-gain planar antennas, IEEE Trans. Antennas and Propagation 53 (1) (2005) 209–215.
[8] A. Ourir, A. de Lustrac, J.-M. Lourtioz, All-metamaterial-based sub-wavelength cavities ($\lambda/60$) for ultrathin directive antennas, Appl. Phys. Lett. 88 (2006) 084103.
[9] D.F. Sievenpiper, J.H. Schaffner, H.J. Song, R.Y. Loo, G. Tangonan, Two-dimensional beam steering using an electrically tunable impedance surface, IEEE Trans. Antennas and Propagation 51 (10) (2003) 2713–2722.
[10] D. F Sievenpiper, Forward and backward leaky wave radiation with large effective aperture from an electronically tunable textured surface, IEEE Trans. Antennas and Propagation 53 (1) (2005) 236–247.
[11] H. Chen, B.-I. Wu, L. Ran, T.M. Grzegorczyk, J.A. Kong, Controllable left-handed metamaterial and its application to a steerable antenna, Appl. Phys. Lett. 89 (2006) 053509.
[12] A. Ourir, A. de Lustrac, J.-M. Lourtioz, Optimization of metamaterial based subwavelength cavities for ultracompact directive antennas, Microwave Opt. Technol. Lett. 48 (12) (2006) 2573–2577.
[13] A. Ourir, S.N. Burokur, A. de Lustrac, Phase-varying metamaterial for compact steerable directive antennas, Electron. Lett. 43 (9) (2007) 493–494.
[14] Microstripes Micro-Stripes Reference Manual Release 7.0, FLOMERICS Ltd., 2005.
[15] G.V. Trentini, Partially reflecting sheet arrays, IRE Trans. Antennas and Propagation 4 (1956) 666–671.